Pressure-induced phonon softenings and the structural and magnetic transitions in CrO_2

Sooran Kim, Kyoo Kim, Chang-Jong Kang, and B. I. Min*

Department of Physics, PCTP, Pohang University of Science and Technology, Pohang, 790-784, Korea

(Received 14 December 2011; published 19 March 2012)

To investigate the pressure-induced structural transitions of chromium dioxide (CrO_2), phonon dispersions and total-energy band structures are calculated as a function of pressure. The observed structural transition has been theoretically reproduced at $P \approx 10$ GPa from the ground-state tetragonal CrO_2 (t-CrO_2) of the rutile type to orthorhombic CrO_2 (o-CrO_2) of the $CaCl_2$ type. The half-metallic property is found to be preserved in o-CrO_2. The softening of the Raman-active B_{1g} phonon mode, which is responsible for this structural transition, is demonstrated. The second structural transition is found to occur for $P \geqslant 61.1$ GPa from ferromagnetic (FM) o-CrO_2 to nonmagnetic monoclinic CrO_2 (m-CrO_2) of the MoO_2 type, which is related to the softening mode at $\mathbf{q} = R(\frac{1}{2},0,\frac{1}{2})$. The third structural transition has been identified at $P = 88.8$ GPa from m-CrO_2 to cubic CrO_2 of the CaF_2 type that is a FM insulator.

DOI: 10.1103/PhysRevB.85.094106 PACS number(s): 63.20.dk, 63.20.D−, 61.50.Ks, 71.15.Nc

I. INTRODUCTION

Chromium dioxide (CrO_2), which crystallizes in the tetragonal structure of the rutile type, is a well-known material because of its half-metallic nature with $T_c = 390$ K.[1] The origin of the ferromagnetic (FM) and half-metallic property of CrO_2 was explained in terms of the double-exchange model.[2,3] Due to the crystal field of distorted (flattened) Cr-O_6 octahedra, Cr t_{2g} states are split into lower d_{xy} and higher d_{xz}/d_{yz} states. Out of two d electrons of Cr^{4+}, one occupies the lower d_{xy} that is localized, while the other occupies the higher d_{xz}/d_{yz} that are delocalized near the Fermi level (E_F) due to the hybridization with O p states. Then the double-exchange interaction arises from the Hund coupling between localized d_{xy} and delocalized half-filled d_{xz}/d_{yz} states, so as to produce the FM and half-metallic properties.

In contrast to numerous reports on electronic and magnetic properties of CrO_2, there has been a relatively small number of studies on structural and lattice dynamical properties of CrO_2. In particular, there is no experimental or theoretical report on the phonon-dispersion curve for CrO_2, except for a few Raman studies.[4–6] Under pressure, CrO_2 is known to undergo the structural transition from the ground-state tetragonal CrO_2 (t-CrO_2) to the orthorhombic CrO_2 (o-CrO_2) of the $CaCl_2$ type at $P = 12$–17 GPa.[4,7] The question that follows is whether there will be additional structural transitions from o-CrO_2 at higher pressure. In fact, this question is not just for CrO_2 but is also relevant to the structural stability issue of transition-metal (TM) dioxides (TMO_2). Note that TMO_2 shows diverse structures depending on the TM elements.[8–11] Furthermore, the magnetic properties of CrO_2 under pressure are intriguing, such as (i) whether the half-metallic nature is preserved, and (ii) when CrO_2 becomes nonmagnetic.

In this work, to investigate the pressure-induced structural transitions of CrO_2, we have studied phonon dispersions and total energies of relevant CrO_2 structures as a function of pressure. Based on the calculated phonon dispersions and the total energies, we have found three possible structural transitions with increasing pressure. The first transition is consistent with the known transition from t-CrO_2 to o-CrO_2. At this transition, FM and half-metallic properties are preserved, in agreement with previous reports in the literature.[4,7] The second transition is from o-CrO_2 to monoclinic CrO_2 (m-CrO_2) of the MoO_2 type, which is nonmagnetic (NM). The third transition is identified from m-CrO_2 to cubic CrO_2 (c-CrO_2) of the CaF_2 type. Interestingly, c-CrO_2 is a FM insulator even at the high pressure of $P \geqslant 88.8$ GPa. Note that the second and third structural transitions are our findings for CrO_2 under the high pressure.

II. COMPUTATIONAL DETAILS

Band structures and phonon dispersions of CrO_2 were obtained by employing the pseudopotential band method and the linear response method, respectively, implemented in the QUANTUM ESPRESSO code.[12,13] The generalized gradient approximation (GGA) is utilized for the exchange-correlation potential. Self-consistent electron and phonon band calculations were carried out after the full relaxation of internal atomic positions and lattice parameters. We have also employed the all-electron full-potential linearized augmented plane-wave (FLAPW) band method,[14] implemented in the WIEN2K package,[15] to check the results from the pseudopotential band method.

We have considered various structures of CrO_2. At the ambient pressure, the stable phase is t-CrO_2 of the rutile type ($P4_2/mnm$), in which Cr atoms are positioned at (0,0,0) and $(\frac{1}{2},\frac{1}{2},\frac{1}{2})$, while O atoms are positioned at $\pm(u,u,0)$ and $\pm(\frac{1}{2}+u, \frac{1}{2}-u, \frac{1}{2})$. Initial lattice constants and atomic positions adopted before the full relaxation are $a = b = 4.421$ Å, $c = 2.916$ Å, and $u = 0.3043$.[16] For the high-pressure phase of o-CrO_2 of the $CaCl_2$ type ($Pnnm$), we have adopted $a = 4.3874$ Å, $b = 4.2818$ Å, $c = 2.8779$ Å, $u_x = 0.299$, and $u_y = 0.272$.[4] For candidate structural phases at the higher pressure, we considered m-CrO_2 of the MoO_2 type ($P2_1/c$)[10,11] and c-CrO_2 of the CaF_2 type ($Fm\bar{3}m$).[17] In the latter, a Cr atom is positioned at (0, 0, 0), and O atoms at (0.25, 0.25, 0.25), (0.25, 0.25, 0.75).

III. RESULTS

Figure 1 shows the phonon dispersions of t-CrO_2 and o-CrO_2 at the ambient and high pressures. As shown in Fig. 1(a), t-CrO_2 at the ambient pressure has regular phonon

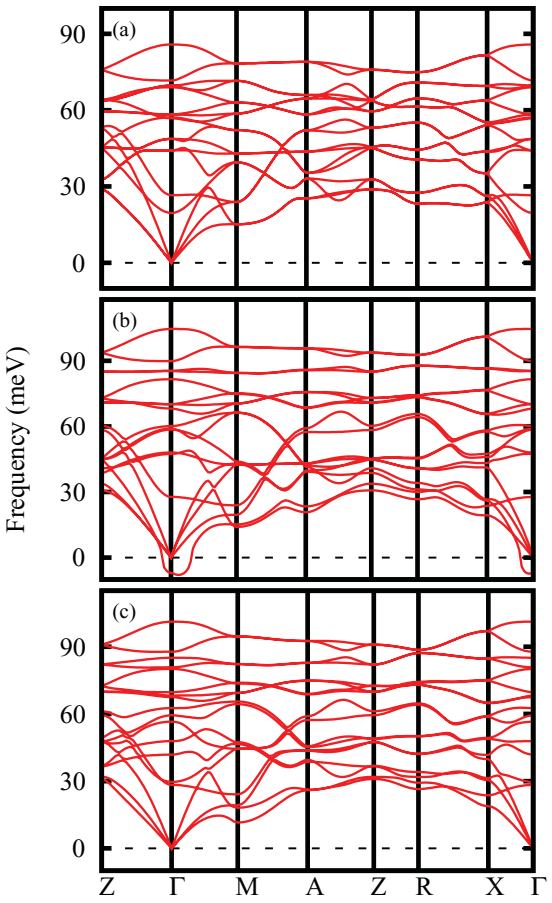

FIG. 1. (Color online) The phonon-dispersion curves of CrO_2. (a) FM t-CrO_2 of the rutile type at the ambient pressure. (b) FM t-CrO_2 at $P = 34.0$ GPa. Notice the phonon softening at Γ, which corresponds to the B_{1g} mode. The negative frequency here represents the imaginary part of the phonon frequency. (c) FM o-CrO_2 of the $CaCl_2$ type at $P = 34.1$ GPa.

dispersions, reflecting the stable phase of t-CrO_2 at the ambient pressure. In contrast, t-CrO_2 at $P = 34.0$ GPa in Fig. 1(b) has a softening phonon mode at $\mathbf{q} = \Gamma$, indicating the structural instability of t-CrO_2 at this pressure. The softened mode corresponds to the B_{1g} mode that is Raman active. As shown in Fig. 2, the B_{1g} mode generates the rotating motions of oxygen ions. The resulting lattice displacements induce the structural transformation from t-CrO_2 of the rutile type to o-CrO_2 of the $CaCl_2$ type. Figure 1(c) provides the phonon dispersion of o-CrO_2 at $P = 34.1$ GPa. The phonon dispersion is regular, implying that o-CrO_2 is stable at this pressure. Therefore, Fig. 1 clearly demonstrates that there is a structural transition from t-CrO_2 to o-CrO_2 at the pressure of $P \leqslant 34$ GPa.

In Fig. 3(a), we plotted the calculated Raman-active phonons of t-CrO_2 and o-CrO_2 as a function of pressure. There are four Raman modes (B_{1g}, E_g, A_{1g}, B_{2g}) for t-CrO_2, and six Raman modes (A_g, B_{1g}, B_{2g}, B_{3g}, A_g, B_{1g}) for o-CrO_2.[4,6,18,19] Our data are consistent with experimental data up to $P \approx 40$ GPa.[4] With an increase in pressure, one can clearly see the softening of the B_{1g} mode of t-CrO_2, which indicates the structural instability of t-CrO_2. One can also notice two transition points. The first one corresponds to the

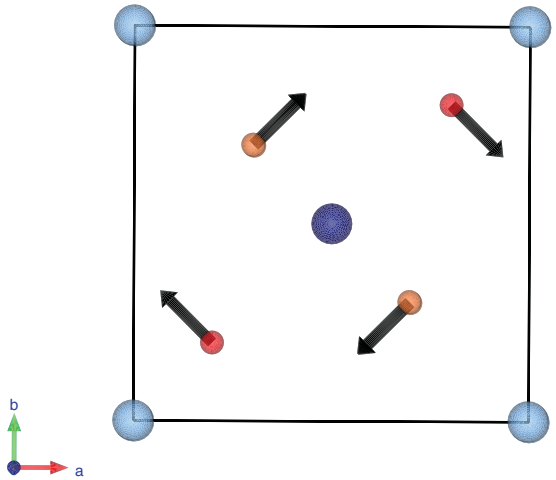

FIG. 2. (Color online) The normal mode of the B_{1g} soft phonon at Γ for $P = 34.0$ GPa. The blue and light-blue circles represent Cr ions, while the orange and red circles (with black arrows) represent oxygen ions. Blue and orange ions are located at $z = \frac{1}{2}$. Only the oxygen ions move in this mode.

transition from t-CrO_2 to o-CrO_2 at $P = 9.8$ GPa. At this transition, CrO_2 keeps its FM and half-metallic properties.[4,7,17] The second one corresponds to the transition at $P = 76.0$ GPa. The stable structure for $P \geqslant 76$ GPa has not been identified yet.

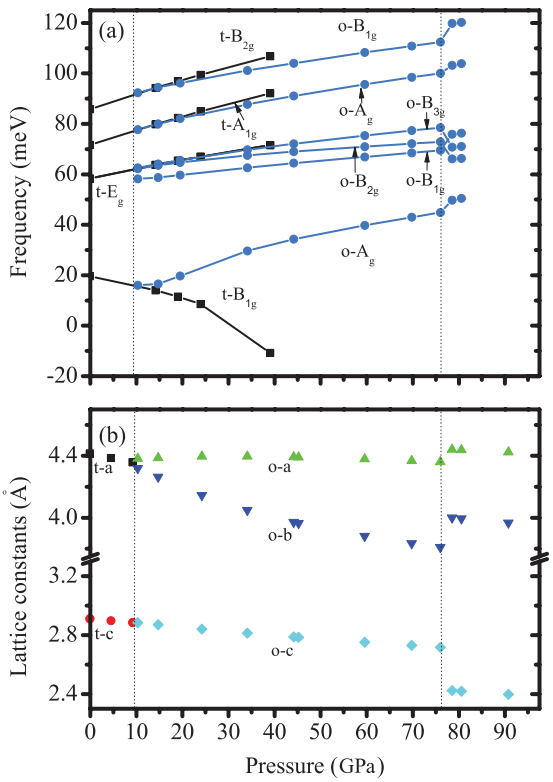

FIG. 3. (Color online) (a) Calculated Raman-active phonon frequencies of t-CrO_2 and o-CrO_2 vs pressure. t- and o- stand for t-CrO_2 and o-CrO_2, respectively. The lines connecting the data are a guide for the eyes. Two phase transitions are noticed at $P = 9.8$ and $P = 76.0$ GPa, which are marked by vertical lines. (b) Calculated equilibrium lattice constants of t-CrO_2 and o-CrO_2 vs pressure.

The phonon anomalies at the two transition points are also revealed in the variation of lattice constants of CrO_2 under pressure. In Fig. 3(b), the lattice constants are plotted as a function of pressure. One can see the anomalous behaviors of the lattice constants at the two transition points that are coincident with those in Fig. 3(a).

To investigate the second structural transition in more detail, we have examined the behavior of the magnetic moment. Srivastava *et al.*[17] once reported that there would be a magnetic transition in t-CrO_2 from half metallic to NM at $P \approx 65$ GPa. However, as discussed above, there occurs a structural transition from t-CrO_2 to o-CrO_2 at the low pressure of about $P = 9.8$ GPa. Hence, in Fig. 4(a), we have examined the magnetic-moment behavior for o-CrO_2. It is seen that there is a FM to NM transition at $P = 76.0$ GPa, which is close to the second structural transition point. The magnetic moment of o-CrO_2 suddenly drops at this transition point ($P = 76.0$ GPa). The half-metallic property persists up to this pressure. This magnetic transition was also observed by Kuznetsov *et al.*,[7] who obtained the transition pressure of $P \approx 53$ GPa by using the pseudopotential band method implemented in the VASP code. It is thus tempting to conjecture that the second transition observed in Fig. 3 corresponds to the magnetic transition in o-CrO_2. However, the phonon-dispersion curve in Fig. 4(b) for NM o-CrO_2 at $P = 80.5$ GPa shows the strong phonon softenings, indicating that even NM o-CrO_2 is unstable at the pressure of $P > 76.0$ GPa. Therefore, it is not possible that FM o-CrO_2 changes into NM o-CrO_2 with an increase in pressure. There might be an additional structural transition in this pressure range.

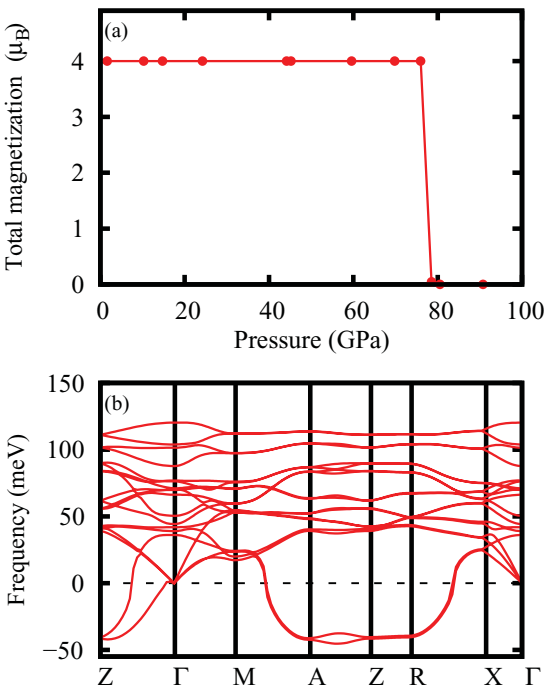

FIG. 4. (Color online) (a) Calculated magnetic moment of o-CrO_2 vs pressure. Magnetic transition from the FM to the NM phase occurs at $P = 76.0$ GPa. (b) The phonon-dispersion curve of NM o-CrO_2 at $P = 80.5$ GPa.

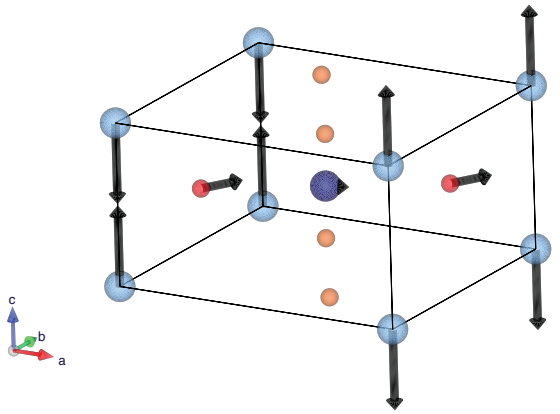

FIG. 5. (Color online) The normal mode of the softened phonon at $\mathbf{q} = R$ for $P = 80.5$ GPa. The blue and light-blue circles represent Cr ions, while the (smaller) orange and red circles represent oxygen ions.

Two candidate structures for $P > 76.0$ GPa are m-CrO_2 of the MoO_2 type and c-CrO_2 of the CaF_2 type. The monoclinic structure of the MoO_2 type is chosen from the expectation that with increasing pressure, two d electrons of Cr become itinerant and the local environment becomes similar to that of MoO_2. Also, TiO_2 and NbO_2 were reported to undergo the structural transitions under high pressure to the monoclinic structure of the baddeleyite type.[20–22] Concerning another candidate, namely, c-CrO_2 of the CaF_2 type, there were previous reports predicting the structural transitions from the $CaCl_2$ type to CaF_2 type for CrO_2[17] and RuO_2.[23] In fact, the CaF_2 type is a typical structure of TMO_2. For example, ZrO_2 and HfO_2, which have relatively large cations, crystallize in a CaF_2-type structure at high temperature.[24,25]

In VO_2, a softening of phonon frequency was observed at $\mathbf{q} = R(\frac{1}{2},0,\frac{1}{2})$, which corresponds to the atomic movements from the tetragonal structure of the rutile type to the monoclinic structure.[26] Indeed, the softening mode at $\mathbf{q} = R$ in Fig. 4(b) is related to this structural transition because the orthorhombic structure of the $CaCl_2$ type is nothing but the distorted

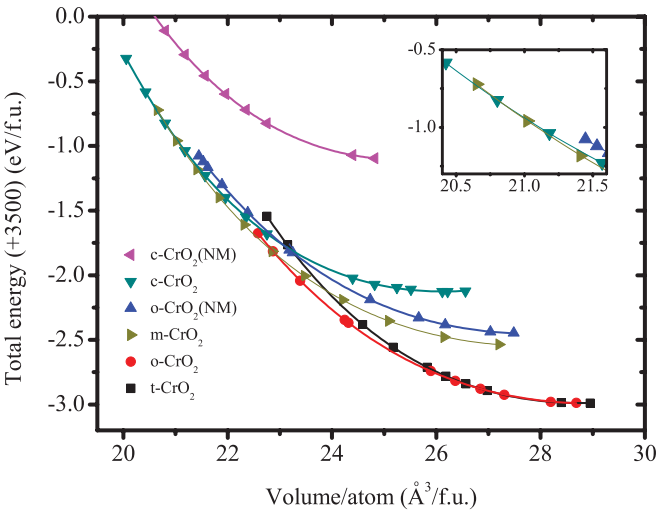

FIG. 6. (Color online) Total energies of various CrO_2 structures vs volume. Data are fitted by the Birch-Murnaghan equation of state.

TABLE I. The fitting parameters of the Birch-Murnaghan equation of state. B_0 is the bulk modulus (units in GPa) and B_0' is its pressure derivative.

	t-CrO_2	o-CrO_2	o-CrO_2 (NM)	c-CrO_2	c-CrO_2 (NM)	m-CrO_2
B_0	236.9	196.9	196.0	255.3	256.6	169.9
B_0'	4.5	3.9	3.8	4.3	4.8	4.8

rutile-type structure. Figure 5 depicts the normal mode of the softened phonon mode at $\mathbf{q} = R$. The displacements generate Cr-Cr dimerization along the c axis, which is consistent with the main distortions of the transition from the rutile type to the monoclinic structure. It is thus reasonable to expect the second transition to be from o-CrO_2 of the $CaCl_2$ type to m-CrO_2 of the MoO_2 type.

To identify the additional structural transition at the higher pressure, we have compared the total energies of the candidate structures. From the total energy vs volume curves in Fig. 6, which are fitted by the Birch-Murnaghan equation of state (see Table I), one can identify three structural phase transitions. The first one is from FM t-CrO_2 to FM o-CrO_2 at the estimated pressure of $P = 12.2$ GPa, which is consistent with the phonon calculation in Fig. 3. For $P \geqslant 61.1$ GPa, NM m-CrO_2 becomes the most stable, which corresponds to the second transition from o-CrO_2 to m-CrO_2, as discussed in the phonon study of Fig. 4. For $P \geqslant 88.8$ GPa, c-CrO_2, which is a FM insulator, becomes the most stable. The more stable FM and insulating phase, compared to the NM metallic phase, of c-CrO_2 at this high pressure is extraordinary. The magnetic moment of c-CrO_2 amounts to $\sim 2\mu_B$/Cr, which is close to those in t-CrO_2 and o-CrO_2. Note, however, that c-CrO_2 is an insulator, not a half metal. We have confirmed this result by the FLAPW band method too. The present result is different from that by Srivastava *et al.*,[17] who obtained the stable NM metallic phase of c-CrO_2 for $P > 90$ GPa. The different result is likely to come from their use of a simple tight-binding linearized muffin-tin orbital (TB-LMTO) band method.

The transition from m-CrO_2 to c-CrO_2 is thought to originate from the increasing packing ratio. There are six and eight oxygens around Cr in m-CrO_2 and c-CrO_2, respectively. Haines *et al.*[23] proposed several possible paths of structural transition from a rutile- to CaF_2-type structure in TMO_2. Interestingly, one of the paths is the same as the present structural transition path: rutile-type ($P4_2/mnm$) $\rightarrow$ $CaCl_2$-type ($Pnnm$) $\rightarrow$ MoO_2-type ($P2_1/c$) $\rightarrow$ CaF_2-type ($Fm\bar{3}m$). But they did not take into account the magnetic state.

IV. CONCLUSION

We have studied the pressure effect on the structural properties of CrO_2 by performing the phonon-dispersion and total-energy band structure calculations. By combining two analysis methods, we have found that there are three structural transitions with increasing pressure up to 100 GPa. The first one is the transition from t-CrO_2 of the rutile type to o-CrO_2 of the $CaCl_2$ type at $P \approx 10$ GPa (9.8 GPa from phonon-dispersion analysis, while 12.2 GPa from the total-energy study). The FM and half-metallic properties of CrO_2 are preserved at this transition. The second structural transition is from FM o-CrO_2 to NM m-CrO_2, which corresponds to the lattice displacement of the phonon softening at $\mathbf{q} = R$ in o-CrO_2. The transition pressure is $P = 76.0$ GPa from the phonon-dispersion analysis, whereas it is $P = 61.1$ GPa from the total-energy study. The third structural transition is from NM m-CrO_2 to FM c-CrO_2 at $P = 88.8$ GPa, which is accompanied by the metal-to-insulator transition.

ACKNOWLEDGMENTS

This work was supported by the NRF (Grants No. 2009-0079947 and No. 2011-0025237), and the KISTI supercomputing center (Grant No. KSC-2011-C2-36). S.K. acknowledges the support from the NRF project of the Global Ph.D. Fellowship program (Grant No. 2011-0002351).

*bimin@postech.ac.kr

[1] K. Schwarz, J. Phys. F **16**, L211 (1986).
[2] M. A. Korotin, V. I. Anisimov, D. I. Khomskii, and G. A. Sawatzky, Phys. Rev. Lett. **80**, 4305 (1998).
[3] M. Katsnelson, V. Irkhin, L. Chioncel, A. Lichtenstein, and R. de Groot, Rev. Mod. Phys. **80**, 315 (2008).
[4] B. R. Maddox, C. S. Yoo, D. Kasinathan, W. E. Pickett, and R. T. Scalettar, Phys. Rev. B **73**, 144111 (2006).
[5] T. Yu, Z. X. Shen, W. X. Sun, J. Y. Lin, and J. Ding, J. Phys. Condens. Matter **15**, L213 (2003).
[6] M. N. Iliev, A. P. Litvinchuk, H.-G. Lee, C. W. Chu, A. Barry, and J. M. D. Coey, Phys. Rev. B **60**, 33 (1999).
[7] A. Y. Kuznetsov, J. S. de Almeida, L. Dubrovinsky, R. Ahuja, S. K. Kwon, I. Kantor, A. Kantor, and N. Guignot, J. Appl. Phys. **99**, 053909 (2006).
[8] L. Mattheiss, Phys. Rev. B **13**, 2433 (1976).
[9] R. Pynn, J. Axe, and R. Thomas, Phys. Rev. B **13**, 2965 (1976).
[10] V. Eyert, R. Horny, K. Hock, and S. Horn, J. Phys. Condens. Matter **12**, 4923 (2000).
[11] V. Eyert, Ann. Phys. (Leipzig) **11**, 650 (2002).
[12] Computer code QUANTUM ESPRESSO (opEn-Source Package for Research in Electronic Structure, Simulation, and Optimization), [http://www.quantum-espresso.org]; P. Giannozzi *et al.*, J. Phys. Condens. Matter **21**, 395502 (2009).

[13]We have used the kinetic-energy cutoff for wave functions of ≈400 eV. We have selected **k**-point samplings, such that we have $8 \times 8 \times 8$ for t-CrO_2 and o-CrO_2, $7 \times 7 \times 5$ for m-CrO_2, and $12 \times 12 \times 8$ for c-CrO_2 in the Monkhorst-Pack grid, to set similar **k**-point density in the Brillouin zone of each structure.

[14]H. J. F. Jansen and A. J. Freeman, Phys. Rev. B **30**, 561 (1984); B. I. Min, H. J. F. Jansen, and A. J. Freeman, *ibid*. **33**, 6383 (1986).

[15]B. Blaha, K. Schwarz, G. K. H. Madsen, D. Kvasnicka, and J. Luitz, computer code WIEN2K (Technische Universität Wien, Austria, 2001).

[16]W. Xue-Wei, N. Dong-Lin, and L. Xiao-Jun, Chin. Phys. Lett. **24**, 3509 (2007).

[17]V. Srivastava, M. Rajagopalan, and S. P. Sanyal, Eur. Phys. J. B **61**, 131 (2008).

[18]S. S. Rosenblum, W. H. Weber, and B. L. Chamberland, Phys. Rev. B **56**, 529 (1997).

[19]W. H. Weber, G. W. Graham, and J. R. McBride, Phys. Rev. B **42**, 10969 (1990).

[20]H. Sato, S. Endo, M. Sugiyama, T. Kikegawa, O. Shimomura, and K. Kusaba, Science (NY) **251**, 786 (1991).

[21]L. Gerward and J. Staun Olsen, J. Appl. Crystallogr. **30**, 259 (1997).

[22]J. Haines, J. M. Léger, A. S. Pereira, D. Häusermann, and M. Hanfland, Phys. Rev. B **59**, 13650 (1999).

[23]J. Haines and J. M. Léger, Phys. Rev. B **48**, 13344 (1993).

[24]A. Muñoz-Páez, J. Chem. Edu. **71**, 381 (1994).

[25]T. V. Perevalov, V. A. Gritsenko, S. B. Erenburg, A. M. Badalyan, and H. Wong, J. Appl. Phys. **101**, 053704 (2007).

[26]F. Gervais and W. Kress, Phys. Rev. B **31**, 4809 (1985).